Calculation of the energy spectrum of a two-electron spherical quantum dot

Calculation of the energy spectrum of a two-electron spherical quantum dot

Ramiro Pino[1] **and Víctor M Villalba**[2]

[1] Department of Mathematics and Computer Science, Technische Universiteit Eindhoven,
PO Box 513, Eindhoven 5600 MB, The Netherlands
[2] Centro de Física, Instituto Venezolano de Investigaciones Científicas, Apartado 21827,
Caracas 1020-A, Venezuela

E-mail: rpino@win.tue.nl and villalba@pion.ivic.ve

Abstract
We study the energy spectrum of the two-electron spherical parabolic quantum
dot using the exact Schrödinger, Hartree–Fock and Kohn–Sham equations. The
results obtained by applying the shifted-$1/N$ method are compared with those
obtained by using an accurate numerical technique, showing that the relative
error is reasonably small, although the first method consistently underestimates
the correct values. The approximate ground-state HF and local-density KS
energies, estimated using the shifted-$1/N$ method, are compared with accurate
numerical self-consistent solutions. We make some perturbative analyses
of the exact energy in terms of the confinement strength, and we propose
some interpolation formulae. A similar analysis is performed for both mean-
field approximations and interpolation formulae are also proposed for these
exchange-only ground-state cases.

1. Introduction

Progress in nanotechnology has allowed the development of small devices, such as quantum
dots. The confinement potential can be safely approximated by a harmonic one [1, 2], which
has boosted the study of quantum dots with parabolic confinement during the last few years
(see e.g. [3] and [4], and references therein). The presence of many interacting electrons
renders the computation of the electronic states and properties a very complicated many-
body problem. The first non-trivial exactly solvable problem of many electrons is that of two
electrons confined in a parabolic potential, which made it a very attractive workbench for
testing all kind of approximations (see e.g. [5–10]).

The Hamiltonian describing the pair of interacting electrons in a parabolic quantum dot in the effective mass approximation can be written as

$$\hat{H} = -\frac{\hbar^2}{2m^*}(\nabla_1^2 + \nabla_2^2) + \frac{1}{2}m^*\omega^2(r_1^2 + r_2^2) + \frac{e^2}{\epsilon|\vec{r}_1 - \vec{r}_2|} \tag{1}$$

where m^* is the effective mass, ω the confinement strength, ϵ the dielectric constant of the host material and ∇^2 the Laplacian operator.

Equation (1) can be separated into a centre-of-mass and a relative motion component. Furthermore, due to the radial symmetry of the components, only those parts of the corresponding Schrödinger equations have to be solved. The centre-of-mass part will give the well-known harmonic oscillator problem. In three dimensions, the relative motion part may admit exact solutions for special choices of the parameters (see e.g. [5]). For the two-dimensional case, similar separation and substitution can be made, and again there are no general solutions expressible in terms of special functions. Nevertheless, in [12], and more recently in [13], it was shown that there exist analytic solutions for special choices of the confinement constant.

Many-body effects are usually divided into exchange and correlation components [14]. Exchange-only effects are considered in Hartree–Fock (HF) and differently in Kohn–Sham (KS) approaches (although in KS the correlation effects can be included), which typically amount to around 10% of the total energy. Correlation is about one order of magnitude smaller. Nevertheless, it has been shown that in two dimensions for two electrons in a harmonic field, correlation may play a bigger role, especially for singlet states (see e.g. [15]).

The shifted-$1/N$ method [16,17] has been applied to various condensed matter problems. Also, the two-dimensional relative motion Schrödinger problem has been solved using this technique in [9,18].

This paper has been structured as follows: in section 2 we describe the Schrödinger, HF and KS approaches we use. In section 3 we solve the exact, HF and KS–LDA equations using an accurate numerical technique and the shifted-$1/N$ method. We also apply perturbation theory up to first order in both limits of confinement for the exact and mean field cases, and we propose some interpolation formulae for the energy. We discuss the accuracy of the mean field approaches, and of the shifted-$1/N$ method for the present case.

2. Method

Throughout the paper the units of energy will be given in terms of the effective Rydberg constant $\mathcal{R}^* = \hbar^2/(2m^*a^{*2})$ and the effective Bohr radius $a^* = \hbar^2\epsilon/m^*e^2$, respectively.

In centre-of-mass and relative coordinates, and measuring in reduced units, the Hamiltonian is

$$\hat{H} = -\left(\frac{1}{4}\nabla_{\vec{R}}^2 + \nabla_{\vec{r}}^2\right) + \gamma^2 R^2 + \frac{\gamma^2}{4}r^2 + \frac{1}{r} \tag{2}$$

where we have chosen the centre-of-mass $\vec{R} = (\vec{r}_1 + \vec{r}_2)/2$ and the relative coordinate $\vec{r} = (\vec{r}_1 - \vec{r}_2)$.

The separation leads to the harmonic oscillator problem for the centre-of-mass coordinate, with energy

$$E_{NL} = \gamma\,(2N + L + 3/2) \tag{3}$$

and eigenfunctions

$$\Psi_{NLM}(\vec{R}) = \mathcal{N}_{NL}\exp\left(-\gamma R^2\right)(2\gamma)^{L/2}R^L L_N^{L+1/2}(2\gamma R^2)Y_{LM}(\theta_R, \phi_R). \tag{4}$$

For the relative coordinate equation the wavefunction can be separated into radial and angular components:

$$\Psi(\vec{r}) = \frac{u(r)}{r} Y_{lm}(\theta, \phi) \tag{5}$$

where $Y_{lm}(\theta, \phi)$ are the spherical harmonics which are eigenfunctions of the angular momentum operator L_z, and L^2 with eigenvalues m and l. This separation makes the corresponding radial Schrödinger equation the following second-order ordinary differential equation:

$$\left[-\frac{d^2}{dr^2} + l(l+1)\frac{1}{r^2} + \frac{1}{4}\gamma^2 r^2 + \frac{1}{r} - E \right] u(r) = 0. \tag{6}$$

It is well known that exact solutions of equation (6) cannot be expressed in a closed form in terms of special functions. There are analytic expressions for the energy for particular values of γ and l, as was pointed out in [5, 11], among others.

The electrons should satisfy the Fermi–Dirac statistics, which means in this case that for singlet states ($s = 0$) the spatial part of the wavefunction should be antisymmetric and for triplet states ($s = 1$) symmetric. As the centre-of-mass coordinate remains the same after exchanging to electrons, the antisymmetry requirement will be in the relative part. Because of the separation in radial and angular components of the relative-coordinate wavefunction it will mean that singlet states are associated with odd l and triplet states with even l, respectively.

It is interesting to compare the results of exact calculations with independent-electron models such as HF and KS [14] in order to assess the relative importance of many-body effects like exchange and correlation, and also to evaluate the performance of the local-density approximation. For two paired electrons the electronic density is $\rho_{HF} = 2|\phi_{HF}|^2$, where ϕ_{HF} is the orbital, and the exchange potential is equal to half of the Hartree one with opposite sign. The HF equation can be written as

$$\left[-\tfrac{1}{2}\nabla^2 + v(r) + \tfrac{1}{2}v_H[\rho_{HF}] \right]\phi_{HF} = \varepsilon_{HF}\, \phi_{HF} \tag{7}$$

where $v(r) = \tfrac{1}{2}\gamma^2 r^2$ and ε_{HF} is the HF orbital energy. The total HF energy is written as

$$E_{HF} = 2\varepsilon_{HF} - \tfrac{1}{2} \int d\vec{r}\, \rho_{HF}\, v_H[\rho_{HF}] \tag{8}$$

where v_H is the Hartree potential given by

$$v_H[\rho] = \int d\vec{r}'\, \frac{\rho(\vec{r}')}{|\vec{r} - \vec{r}'|}. \tag{9}$$

The KS equation can be written as

$$[-\tfrac{1}{2}\nabla^2 + v(r) + v_H[\rho_{KS}] + v_x(\rho_{KS})]\phi_{KS} = \varepsilon_{KS}\, \phi_{KS} \tag{10}$$

where ε_{KS} and ϕ_{KS} are the KS orbital energy and eigenfunction, respectively, and again $\rho_{KS} = 2|\phi_{KS}|^2$. We take here the local-density approximation for which $v_x(\rho) = \tfrac{4}{3}c_x\rho^{1/3}$, with $c_x = -\tfrac{3}{4}\left(\tfrac{3}{\pi}\right)^{1/3}$ (see e.g. [14]). The total KS energy is given by

$$E_{KS} = 2\varepsilon_{KS} - \tfrac{1}{2} \int d\vec{r}\, \rho_{KS}\, v_H[\rho_{KS}] - \tfrac{1}{3} \int d\vec{r}\, \rho_{KS}\, v_x(\rho_{KS}). \tag{11}$$

Equations (7) and (10) have asymptotics controlled by the harmonic potential, so the asymptotic density looks like

$$\rho_a(\vec{r}) \propto \exp\left(-\gamma r^2\right). \tag{12}$$

3. Results and discussion

First we make an analysis of the solution of the exact case using the $1/N$ approximation. For details of the derivation of the formulae related to the shifted-$1/N$ method, we refer to the literature (see e.g. [9, 16–18]).

In order to establish the accuracy of the results obtained by the application of the shifted-$1/N$ method we compare them with those obtained by using the Schwartz numeric method [19]. The method is based on a numerical approximation of functions on a mesh and gives very accurate results [20, 21]. There are only empirical estimates of the error [19], which turns out to be exponentially decaying with the number of points given on the mesh step. The interpolation function is chosen as

$$f(r) = \sum_m f_m \frac{u(r)}{(r - r_m)a_m} \tag{13}$$

where

$$u(r) = \sin[\pi(r/h)^{1/2}]. \tag{14}$$

Here r_m is a zero of $u(r)$, a_m is a zero of its derivative and h is the step of the mesh, which turns out to be quadratically spaced.

The choice of the step h was made after estimating the characteristic length of the effective potential, and then multiplying the obtained estimate by five and dividing it by the square of the number of points in the mesh, usually around 300. This guarantees that h is minimal for a given ω, and also that the function value at the last mesh point is practically zero.

In figure 1 we show the behaviour of the error of the energy of the few lowest eigenvalues calculated using the shifted-$1/N$ method, compared with the accurate results obtained using the Schwartz method. We plotted the relative error, defined as $\delta E = E_{\text{approx}}/E_{\text{exact}} - 1$, as a function of the reduced variable $\gamma' = \gamma/(\gamma + 1)$. The 0s, 0p, and 0d states are the three lowest energy states of the relative motion with angular momentum $l = 0, 1$ and 2, respectively. It can be seen that the error remains bounded in 0.5% for the first eigenvalue, in 0.075% for the second one and 0.022% for the third one. It is noticeable that the method always underestimates the correct values of the energy, and that the error decreases with the increase in the angular quantum number l, as should be expected. Furthermore, the error has some maximum between the two limiting cases, after which it decreases as expected, since the shifted-$1/N$ method reproduces exactly the oscillator case.

Figure 2 shows the behaviour of the total energy (the sum of the centre-of-mass and relative motion energies) as a function of γ', as calculated using the shifted-$1/N$ method. The first two symbols are the indices of the centre-of-mass component of the energy, and the last two correspond to the relative motion. The lowest six states are depicted. The inset is a magnification for γ' from 0.01 to 0.15. Here, an apparent linear behaviour can be observed, but a more careful analysis indicates that, for instance, for the ground-state first 6–8 points, the effective power in terms of γ' is about 0.8. For the last few points the curve can be fitted well with a function of the type $\gamma'/(1 - \gamma')$, which is the expected behaviour for electrons in a harmonic field. The relative error is not shown, but it is estimated to be roughly one half of the one shown in figure 1, since the centre-of-mass energy can be calculated exactly and it is typically of the size of the relative motion energy.

Although we are able to solve the Schrödinger equation very accurately for this system, perturbation analysis can give some more insight into the behaviour of the electrons under weak and strong confinement. For weak confinement ($\gamma \rightarrow 0$) we have that the kinetic energy term can be neglected (see e.g. [13, 22]), which corresponds to the strong interaction limit
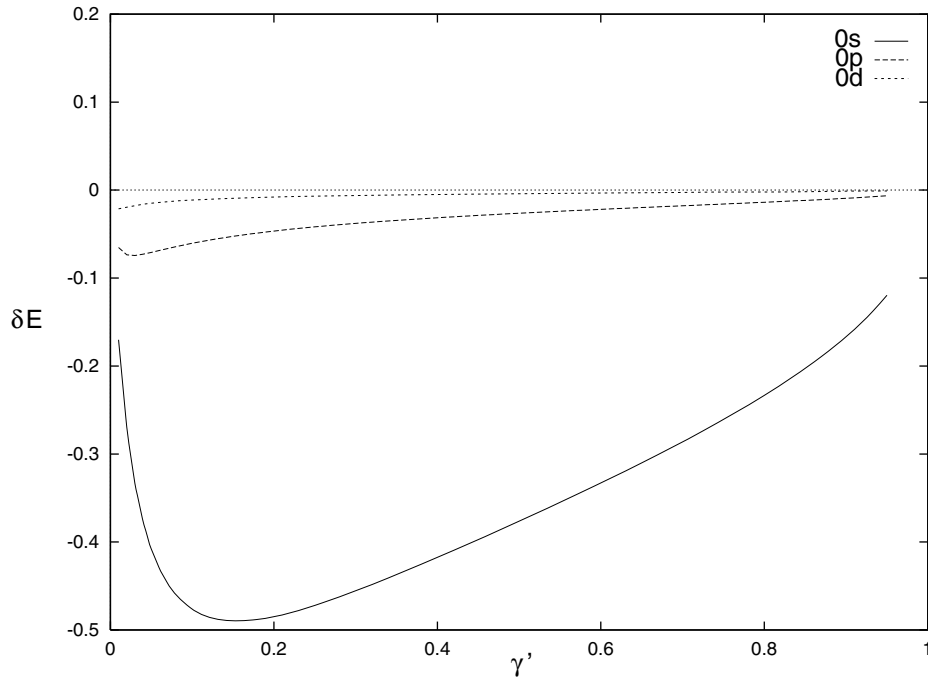
Figure 1. Relative error ($\delta E = (E_{1/N}/E_{\text{exact}} - 1) \times 100$) of the energy of the relative motion for the lowest energy states for $l = 0, 1$ and 2 calculated with the $1/N$ method as a function of the reduced frequency $\gamma' = \gamma/(\gamma + 1)$.

(Wigner crystallization). Then, the energy is approximately taken as the minimum of the effective potential (this is the zeroth-order approximation to the energy):

$$V_l(r) = l(l+1)\frac{1}{r^2} + \frac{1}{4}\gamma^2 r^2 + \frac{1}{r}. \tag{15}$$

The minimum is reached for r_0^l that satisfies the equation

$$\gamma^2 r_0^{l\,4} - 2r_0^l - 4l(l+1) = 0. \tag{16}$$

For $l = 0$ $r_0^0 = (2/\gamma^2)^{1/3}$ and for $l \gg \gamma/2$ $r_0^l \approx (2l/\gamma)^{1/2}$. The minimum of the potential is then

$$U_0^l = l(l+1)\frac{1}{r_0^{l\,2}} + \frac{1}{4}\gamma^2 r_0^{l\,2} + \frac{1}{r_0^l} \tag{17}$$

which is $2^{-1/3}3/2\gamma^{2/3}$ for $l = 0$ and $\gamma(2l+1)/2 + \gamma^{1/2}/(2l)^{1/2}$ for large enough values of l.

The next order in the approximation is to get the effective frequency $\gamma_l^2 = \frac{1}{2}\,\mathrm{d}^2 V_l(r)/\mathrm{d}r^2|_{r=r_0^l}$:

$$\gamma_l^2 = \frac{1}{4}\gamma^2 + \frac{1}{r_0^{l\,3}} + \frac{3l(l+1)}{r_0^{l\,4}} \tag{18}$$

which is $\gamma_0^2 = 3/4\gamma^2$ and $\gamma_l^2 = \gamma^2 + 3/4\gamma^2/l + 2^{1/2}/4(\gamma/l)^{3/2}$ for large l. Now we can estimate the energy levels of this effective harmonic field. So the total energy in the weak confinement limit is

$$E_{nl} \approx l(l+1)\frac{1}{r_0^{l\,2}} + \frac{1}{4}\gamma^2 r_0^{l\,2} + \frac{1}{r_0^l} + 2\gamma_l(n + 1/2) \tag{19}$$
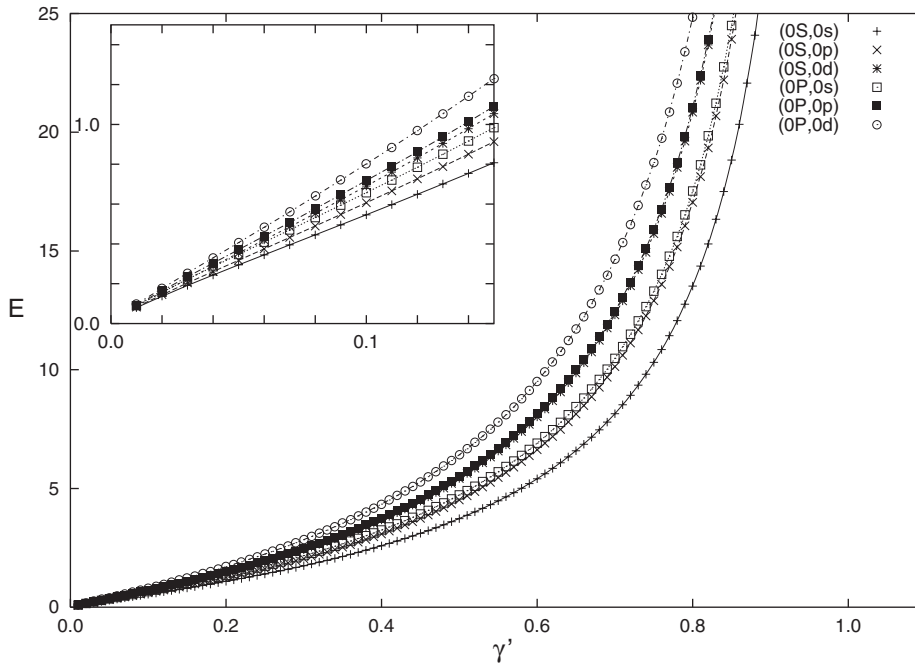
Figure 2. Total energy as a function of $\gamma' = \gamma/(\gamma + 1)$ for the few lowest energy states. $0S$, and $0P$ depict the lowest energy states for the centre-of-mass motion for $L = 0$ and 1, respectively, and 0s, 0p and 0d the lowest energy states for the relative motion for $l = 0$, 1 and 2, respectively. The inset shows a magnification for small γ'.

where $n = 0, 1, \ldots$. For $l = 0$

$$E_{n0} \approx \frac{3}{2} 2^{-1/3} \gamma^{2/3} + \frac{3^{1/2}}{2} \gamma \left(n + \frac{1}{2} \right). \tag{20}$$

For l large enough

$$E_{nl} \approx \frac{1}{2} \gamma (2l + 1) + \left(\frac{\gamma}{2l} \right)^{1/2} + 2 \left[\gamma^2 + \frac{3}{4} \frac{\gamma^2}{l} + \frac{2^{1/2}}{4} \left(\frac{\gamma}{l} \right)^{3/2} \right]^{1/2} \left(n + \frac{1}{2} \right). \tag{21}$$

Equation (20) gives the explanation of why the effective power of the ground-state energy for small γ' is approximately 0.8: it is between 2/3 and 1, the effective powers for the weak field limit for the relative motion and the centre-of-mass energies in terms of $\gamma' \approx \gamma$.

In the strong confinement regime, the zeroth-order approximation amounts to neglecting the electron–electron interaction, so it corresponds to the oscillator's energy. Application of the first order of the perturbation theory [23] for strong confinement ($\gamma \to \infty$) for the relative coordinate equation leads to

$$E_{nl} \approx E_{nl}^{\mathrm{osc}} + \langle \phi_{nl}^{\mathrm{osc}} | r^{-1} | \phi_{nl}^{\mathrm{osc}} \rangle \tag{22}$$

where $E_{nl}^{\mathrm{osc}} = 2\gamma (2n + l + \frac{3}{2})$ and substituting ϕ_{nl}^{osc} (which is similar to equation (4)) into the above equation gives

$$E_{nl} \approx 2\gamma (2n + l + 3/2) + \frac{\gamma^{1/2}}{2^{1/2}} \sum_{k,k'=0}^{n} a_{nl,2k} a_{nl,2k'} \Gamma(l + k + k' + 1) \mathcal{N}_{nl}^2 \tag{23}$$

where $a_{nl,2k}$ are the coefficients of the generalized Laguerre polynomials (of equation (4)) that satisfy the recursion

$$a_{nl,2k} = a_{nl,2(k-1)} \frac{k-n-1}{k(k+l+\frac{1}{2})} \tag{24}$$

with $a_{nl,0} = 1$. Furthermore, the normalization constant is given by

$$\mathcal{N}_{nl}^{-2} = \sum_{k,k'=0}^{n} a_{nl,2k} a_{nl,2k'} \Gamma(l + k + k' + \tfrac{3}{2}). \tag{25}$$

Based on the perturbative results of equations (17), (19) and (23) we propose the following interpolation formula:

$$E_{nl}^{(\mathrm{int})}(\gamma) = \frac{\gamma^{-1} E_{nl}^{(0)} + \gamma E_{nl}^{(\infty)}}{\gamma^{-1} + \gamma} \tag{26}$$

where the superscripts (0) and (∞) correspond to the zero and infinite confinement limits. For $\gamma \to 0$ equation (26) will return approximately the weak confinement limit and for $\gamma \to \infty$ the strong confinement limit. For the zeroth-order approximations equation (26) leads to

$$E_{nl}^{(\mathrm{int})}(\gamma) = \frac{\gamma^{-1} U_0^l + 2\gamma^2 (2n + l + \frac{3}{2})}{\gamma^{-1} + \gamma} \tag{27}$$

and for the first-order pertubative results it will be

$$E_{nl}^{(\mathrm{int})}(\gamma) = \frac{\gamma^{-1}[U_0^l + 2\gamma_l(n + \frac{1}{2})] + \gamma[2\gamma(2n + l + \frac{3}{2}) + 2^{-1/2}\gamma^{1/2}\Delta_{nl}]}{\gamma^{-1} + \gamma} \tag{28}$$

where Δ_{nl} denotes the summation on the right-hand side of equation (23). The interpolation scheme of equation (27) performs consistently badly, except for the very weak and very strong fields. The error goes up to 41% for the ground state, underestimating the correct values. The introduction of first-order corrections, corresponding to the interpolation scheme of equation (28), brings a dramatic improvement on the values: for the ground state the relative error is never worse than 3.3% for the energy of the relative motion, which means that the relative error of the total energy is around 1.7%.

In the case of the mean-field approximations like HF and KS, we have considered the paired-electron ground-state case, and since the confining potential is radially symmetric, the orbitals and the density are also radially symmetric. We implemented the shifted-$1/N$ technique for the HF and KS equations. Here, a word about accuracy is needed: although the solution of the Schrödinger-like equations using the Schwartz method is very accurate, the estimate of the Hartree potential is not as accurate anymore: nevertheless, five to six figures are always guaranteed. The results are shown in table 1 in the first and third columns, indicated as HF-$1/N$ and KS-$1/N$, respectively. Since the resulting wavefunction from the application of the $1/N$ has a complicated form which makes a direct evaluation of the density or of the Hartree potential difficult, we assumed, as an initial guess, the non-interacting density, which is also correct asymptotically. For comparison purposes, we have again used the Schwartz technique self-consistently to solve both the HF and KS equations. Numerical results are shown in the second and fourth columns of table 1, indicated as HF-num and KS-num, respectively. Also, for comparison purposes, we included the results of solving the full Schrödinger equation using the shifted-$1/N$ method and the numeric solution, which are the last two columns, indicated as Exact-$1/N$ and Exact-num, respectively.

Table 1 shows very good agreement between the results from the accurate numerical result and the ones calculated with the $1/N$ method. We should not be too enthusiastic about the

Table 1. Three-dimensional two-electron quantum dot total energy, using the HF, KS and exact Schrödinger (Exact) equations for selected values of the reduced confinement constant (γ'), calculated using the shifted-$1/N$ ($1/N$) and Schwartz numeric (num) methods.

γ'	HF-$1/N$	HF-num	KS-$1/N$	KS-num	Exact-$1/N$	Exact-num
0.1	0.5666	0.5768	0.5960	0.6082	0.5443	0.546 06
0.2	1.1163	1.1241	1.1644	1.1742	1.0858	1.089 26
0.3	1.7758	1.7826	1.8408	1.8503	1.7398	1.744 78
0.4	2.6200	2.6255	2.7029	2.7118	2.5791	2.585 69
0.5	3.7673	3.7717	3.8711	3.8791	3.7217	3.730 12
0.6	5.4477	5.4508	5.5775	5.5842	5.3972	5.407 75
0.7	8.1906	8.1922	8.3558	8.3608	8.1345	8.147 78
0.8	13.5693	13.5693	13.7902	13.7928	13.5057	13.523 2
0.9	29.3703	29.3679	29.7094	29.7082	29.2930	29.319 4

accuracy, since the remarkable agreement is probably a result of the compensation of errors from the calculation of the Hartree potential and energy (due to its simplicity) and the intrinsic error of the $1/N$ method, especially for the weak field case. It can also be seen that the relative accuracy improves from typically a few times 10^{-2} to $10^{-4} - 10^{-5}$ with the increase in the strength of the field. Also the systematic difference between the HF and KS methods is reduced with stronger confinement. Both behaviours can be understood by taking into account that the confinement potential dominates over the decaying electron–electron interaction potential, and with the increase of the strength of confinement the problem becomes just a harmonic potential problem, for which the shifted-$1/N$ is designed to give the exact energy, although the quality of the wavefunction is not too good.

In order to better understand the behaviour of the pair of electrons in strong and weak confinement within these mean-field theories, we can have recourse to pertubation analysis. In the strong confinement limit ($\gamma \to \infty$) the system will behave basically as a pair of non-interacting electrons, and the electron–electron interaction (Hartree and exchange potentials) can be considered as a perturbation. The HF and KS orbitals become

$$\phi(\vec{r}) = \left(\frac{\gamma}{\pi}\right)^{3/4} \exp\left(-\frac{1}{2}\gamma r^2\right) \tag{29}$$

so the Hartree energy will be $2(2\gamma/\pi)^{1/2}$ and the LDA exchange $3c_x 2^{1/3}(3\gamma/\pi)^{1/2}/4$. Then the total HF energy will be

$$E_{\mathrm{HF}}^{(\infty)} = 3\gamma + \left(\frac{2\gamma}{\pi}\right)^{1/2} \tag{30}$$

and the total KS energy

$$E_{\mathrm{KS}}^{(\infty)} = 3\gamma + \left(2^{3/2} + \frac{3}{4}2^{1/3}3^{1/2}c_x\right)\left(\frac{\gamma}{\pi}\right)^{1/2}. \tag{31}$$

In the weak confinement limit ($\gamma \to 0$), due to scaling arguments, we can neglect the kinetic energy, and we can assume constant density, at least within a certain radius R (this is asymptotically true for the HF approximation and arguably for the KS one). Now, taking equations (7) and (10), and using Poisson's equation, we get that $\rho_{\mathrm{HF}} \approx \gamma^2/(2\pi)$ and $\rho_{\mathrm{KS}} \approx \gamma^2/(4\pi)$. Then from the normalization condition $R = [3/(2\pi\rho)]^{1/3}$. The Hartree potential will take the form

$$v_{\mathrm{H}}(r) = \frac{3}{R} - \frac{r^2}{R^3} \qquad \text{if} \quad r \leqslant R \tag{32}$$

and $v_H(r) = 2/r$ if $r \geqslant R$. The Hartree energy will be equal to $12/(5R)$. Substituting the above result into equation (8) we get that the HF energy will be

$$E_{\text{HF}}^{(0)} \approx (3\gamma)^{2/3}. \tag{33}$$

Substituting the result for the Hartree energy into equation (11) we find that in this limit the KS energy will be equal to

$$E_{\text{KS}}^{(0)} \approx \gamma^{2/3} \left(6^{3/2} + \frac{2c_x}{5(4\pi)^{1/3}} \right). \tag{34}$$

Again, we can use interpolation schemes like that of equation (26), so that for the HF ground-state energy we will have

$$E_{\text{HF}}^{(\text{int})}(\gamma) \approx \frac{(3\gamma)^{2/3} + \gamma^2[3\gamma + (2\gamma/\pi)^{1/2}]}{1 + \gamma^2}. \tag{35}$$

In the KS case we can write down

$$E_{\text{KS}}^{(\text{int})}(\gamma) \approx \frac{\gamma^{2/3}[6^{3/2} + 2c_x/5/(4\pi)^{1/3}] + \gamma^2[3\gamma + (2^{3/2} + 3\,2^{1/3}3^{1/2}c_x/4)(\gamma/\pi)^{1/2}]}{1 + \gamma^2}. \tag{36}$$

Comparing the asymptotics of the exact equation for the ground state in the strong confinement limit with the asymptotics of the HF equation, we observe that they coincide. In the KS case the zeroth order is the same, but the coefficient of the first-order perturbation is slightly higher (1.62 compared to the exact $\sqrt{2} \approx 1.41$). In the low density limit (weak confinement), although the three asymptotes are proportional to $\gamma^{2/3}$ in the zeroth order, the coefficients differ substantially: the exact is 1.19, the HF 2.08 and the KS 3.17. This indicates a consistent overestimation of the energy by the independent-electron approximations, which is the expected behaviour, at least for the HF approximation. Our findings for this system for the weak and strong asymptotics, and the numerical results, suggest that KS–LDA energies are always higher than the HF energies, which is consistent with numerical experience on atoms and molecules [14]. From the results shown in table 1 we can estimate the correlation energies for the ground state for different confinement strengths. For $\gamma' = 0.1$, the correlation energy is about 5.6% of the total energy, while for $\gamma' = 0.9$ (strong confinement) it is about 0.17% (for the lightest many-electron atom, helium, it is about 1.4%, and for argon with $Z = 18$, it is only 0.14%). This adds evidence to the suggestion that, for harmonic fields, correlation effects are more important, also in three dimensions, especially for weak confinement.

4. Concluding remarks

In the present paper we have calculated the energy spectrum of a two-electron spherical quantum dot for the few lowest states, using the shifted-$1/N$ method and the very accurate numerical Schwartz method. From comparison of the numerical results we could assess the quality of the shifted-$1/N$ method, which consistently underestimates the correct values, although the error is rather small, and it decreases with the increase of the relative angular momentum. We have also applied perturbation theory up to first order in both limits of confinement of the electron, and we have proposed some interpolation formulae for the energy. Inclusion of first-order perturbation allowed us to construct an interpolation expression that performs reasonably well. We also solved the mean-field HF and local-density KS problems for the ground state. Using the shifted-$1/N$ method we went from reasonable to high accuracy already in the first iteration, compared to the self-consistent numeric solution using the Schwartz method. We made an analysis of the strong and weak confinement limits, and proposed interpolation formulae for both the HF and KS ground-state energies. It was shown that the correlation energy is relatively large for this system, especially for weak confinement.

Acknowledgment

References

[1] Sikorski Ch and Merkt U 1989 *Phys. Rev. Lett.* **62** 2164
[2] Peeters F M 1990 *Phys. Rev.* B **42** 1486
[3] Beenakker C W J 1997 *Rev. Mod. Phys.* **69** 731
[4] Johnson N F 1995 *J. Phys.: Condens. Matter* **7** 965
[5] Kais S, Herschbach D R and Levine R D 1989 *J. Chem. Phys.* **91** 7791
[6] Lamouche G and Fishman G 1998 *J. Phys.: Condens. Matter* **10** 7857
[7] Dineykahn M and Nazmitdinov R G 1997 *Phys. Rev.* B **55** 13 707
[8] Zhu J L, Li Z Q, Yu J Z, Ohno K and Kawazoe Y 1997 *Phys. Rev.* B **55** 15 819
[9] El-Said M 1995 *J. Phys. I (France)* **5** 1027
[10] Mikahilov I D and Betancur F J 1999 *Phys. Status Solidi* b **213** 325
[11] Kestner N R and Sinanoglu O 1962 *Phys. Rev.* **128** 2687
[12] Lozanskii E D and Firsov O B 1974 *Izv. Vyssh. Uchebn. Zaved. Fiz.* **6** 52
[13] Taut M 1993 *Phys. Rev.* A **48** 3561
[14] Parr R G and Yang W 1989 *Density-Functional Theory of Atoms and Molecules* (New York: Oxford University Press)
[15] Pfannkuche D, Gudmundsson V and Maksym P A 1993 *Phys. Rev.* B **47** 2244
[16] Imbo T, Pagnamenta A and Sukhatme U 1984 *Phys. Rev.* D **29** 1669
[17] Imbo T and Sukhatme U 1985 *Phys. Rev.* D **31** 2655
[18] El-Said M 2000 *Phys. Rev.* B **61** 13026
[19] Schwartz C 1985 *J. Math. Phys.* **26** 411
[20] Villalba V M and Pino R 1996 *J. Phys.: Condens. Matter* **8** 8067
[21] Pino R and Villalba V M 1999 *Phys. Status Solidi* b **211** 641
[22] González A 1997 *J. Phys.: Condens. Matter* **9** 4643
[23] Davydov A S 1965 *Quantum Mechanics* (Oxford: Pergamon)